Exploiting Anchor Links for NLOS Combating in UWB Localization

YIJIE CHEN, Tsinghua University, Beijing, China
JILIANG WANG, Tsinghua University, Beijing, China
JING YANG, Tsinghua University, Beijing, China

UWB (Ultra-wideband) has been shown to be a promising technology to provide accurate positioning for the Internet of Things. However, its performance significantly degrades in practice due to Non-Line-Of-Sight (NLOS) issues. Various approaches have implicitly or explicitly explored the problem. In this article, we propose RefLoc, which leverages the unique benefits of UWB to address the NLOS problem. While we find that NLOS links can vary significantly in the same environment, LOS links possess similar features that can be captured by the high bandwidth of UWB. Specifically, the high-level idea of RefLoc is to first identify links among anchors with known positions and leverage those links as references for tag link identification. To achieve this, we address the practical challenges of deriving anchor link status, extracting qualified link features, and inferring tag links with anchor links. We implement RefLoc on commercial hardware and conduct extensive experiments in different environments. The evaluation results show that RefLoc achieves an average NLOS identification accuracy of 96% in various environments, improving the state-of-the-art by 10%, and reduces 80% localization error with little overhead.

CCS Concepts: • **Networks → Location-based services**; • **Human-centered computing → Ubiquitous and mobile computing;**

Additional Key Words and Phrases: UWB localization, NLOS, link identification, environment adaptability

ACM Reference Format:
Yijie Chen, Jiliang Wang, and Jing Yang. 2024. Exploiting Anchor Links for NLOS Combating in UWB Localization. *ACM Trans. Sensor Netw.* 20, 3, Article 72 (May 2024), 22 pages. https://doi.org/10.1145/3657639

1 INTRODUCTION

UWB (Ultra-wideband) has been increasingly recognized as a promising localization technology. Thanks to its high bandwidth, it can achieve decimeter-level or even higher localization accuracy. There has been a large collection of research on UWB localization and its applications, such as robot navigation [56], sports analysis [27], backscatter [59] and concurrent ranging [28]. Further, many commercial systems have sprung up, e.g., Dimension4 by Ubisense [2], Humatics by Time Domain [3], and Airtags by Apple [7].

This work is in part supported by the National Key R&D Program of China (grant no. 2022YFC3801300) and the National Natural Science Foundation of China (grant nos. U22A2031, 61932013, 62172250).
Authors' addresses: Y. Chen, J. Wang (Corresponding author), and J. Yang, School of Software, Tsinghua University, Beijing, China; e-mails: cyj20@mails.tsinghua.edu.cn, jiliangwang@tsinghua.edu.cn, jing-yan18@mails.tsinghua.edu.cn.

ACM 1550-4859/2024/05-ART72
https://doi.org/10.1145/3657639

UWB is promising to achieve accurate localization and is much more resilient to multipath and interference than narrowband **radiofrequency (RF)** technologies such as Bluetooth and WiFi [30, 40, 55]. The basic idea of UWB localization is to measure the distance from UWB tags (i.e., localization targets) to pre-deployed UWB anchors, and then localize tags using ToA, TDoA, etc. [9, 17, 29, 35, 76]. However, its performance significantly degrades in real environments with **Non-Line-Of-Sight (NLOS)** issues, e.g., when people or obstacles block the link. The NLOS problem introduces a high-ranging error due to difficulty in estimating the correct **Line-Of-Sight (LOS)** path [4] and becomes one of the major issues hampering the applications of UWB localization. In practice, NLOS is supposed to happen frequently, e.g., when a human or a robot carrying a UWB device moves around in buildings.

Many localization approaches can explicitly or implicitly address the NLOS problem [25, 41, 82]. For example, one common solution is first to identify the link status (i.e., LOS or NLOS) and then discard the NLOS link or mitigate its impact on localization. Typical methods rely on prior knowledge to identify link status with extensive measurements, e.g., ranging distributions, to identify NLOS links [13, 20, 22, 33, 57, 82, 85, 91]. The authors of [20] propose a graph-based method to implicitly address the NLOS problem, but it requires offline data collection before application to infer accurate multi-modal noise distributions. There are also plenty of one-step solutions that leverage empirical parameters [5, 10, 11, 24, 32, 42, 46]. The methods in both [42] and [32] use a metric related to the received signal power and the first-path power and infer a threshold for NLOS link identification. These methods, however, may fail to adapt to different environments and hardware due to a single threshold. Recent works propose to use machine learning [12, 25, 36, 48, 51, 52, 60, 62, 65, 67, 77, 86] for link identification. Though they can obtain encouraging results, they require large amounts of data for training that involves expensive labor costs and also faces the environmental adaptation problem.

In this article, we propose RefLoc to address the NLOS problem in UWB localization without a prior site survey. The high-level idea is to leverage the links among known anchors as references to identify links for tags. Given the high bandwidth and rich features of UWB, we find that LOS links can exhibit similar features thanks to the tolerance to multipath, while NLOS links may vary significantly in the same environment (e.g., in the same room). We analyze and verify this observation in Section 2.4. More specifically, we propose a low-cost, ranging-based method for anchor link identification. Next, we quantify and extract effective features to represent link status and use them to infer LOS and NLOS tag links. Then, we improve the localization accuracy based on the inferred link status. In this way, RefLoc can adapt to different environments without prior data collection and training.

We address the following challenges in the practical design of RefLoc on commodity UWB devices.

(1) *How to identify the link status of anchors at a low cost?* Intuitively, we can infer the anchor link status based on the ranging results among anchors and the known locations of anchors since a larger ranging error indicates a higher probability of an NLOS link. However, dedicated ranging for anchors introduces additional energy and delays [19, 35, 76, 88]. To make things worse, the link status of anchors can also vary across environments and time. For instance, a person's movement can dynamically turn LOS links into NLOS links or vice versa. To address the problem, we propose an overhearing-based method to infer the anchor link status, which significantly reduces the overhead by only overhearing packets during the tag-ranging process.

(2) *How to select effective link features to identify links?* In the literature, we can find plenty of link features to model the link status. However, not all features can capture the essential difference of UWB LOS/NLOS links considering its super multipath resolution ability. Therefore, we should identify which features are effective for UWB links and how to fuse these features for

link identification. We thus manage to rank the feature quality in terms of link identification. We give higher confidence to highly ranked features so that we can combine high-quality features to improve performance. Specifically, we investigate different features and leverage a Chi-Square test method to estimate the feature quality. We then select effective features and infer corresponding confidence metrics based on the feature quality. Furthermore, we can leverage real-time anchor link features in the environment to identify tag links, thus ensuring environmental adaptability.

(3) *How to effectively identify LOS/NLOS tag links with referenced anchor links?* Basically, we can classify tag links into two groups (e.g., by clustering) as LOS and NLOS links should exhibit different behaviors. However, we show that the accuracy can be low due to two reasons: (i) The data are sparse, e.g., there are only three packets—i.e., three **channel impulse responses (CIRs)**—for link identification in a ranging process. (ii) The data are biased, e.g., the feature of LOS links should be close to each other in the group due to link similarity, whereas the NLOS data can be very different from each other. This makes the classification of two groups very difficult. Therefore, we design a multi-dimensional clustering method that exploits consecutive measurement packets and feature combinations to enrich data as much as possible. To address data bias, instead of directly deriving the LOS link, we iteratively filter out NLOS links far from the LOS links to achieve reliable link identification.

After link identification, we adopt a **Taylor Series (TS)** based **Least-Square (LS)** algorithm [18, 81] for localization, which iteratively calibrates the NLOS ranges and updates the target position with low costs. We conduct comparative experiments to show its efficiency in terms of both time and localization accuracy. Finally, we propose a localization-based method to validate the identification results and deal with misidentifications.

Main results and contributions:

- We propose to leverage anchor links as a reference to address the NLOS links for UWB localization without prior measurements and maintain environment adaptability. We show that NLOS links may vary significantly even in the same environment whereas LOS links can possess similar features no matter what position by exploiting rich features in the high bandwidth of UWB.
- We propose the design of RefLoc and implement it on commercial hardware. We address several practical challenges. We also apply RefLoc to a real system and design a UWB badge (see Figure 11) for people-tracking applications.
- We conduct extensive evaluations in various environments. The results show that RefLoc achieves an average NLOS identification accuracy of 96%, improving accuracy 10% compared with the state-of-the-art. RefLoc achieves a 90% error of 0.42 m in NLOS conditions which reduces the localization error by 80%.

2 BACKGROUND AND MOTIVATION

2.1 Motivation

Location information plays a critical role in location-based services. We can obtain accurate location information outdoors through **global navigation satellite systems (GNSSs)**. However, in indoor environments, the positioning error of GNSS-based positioning methods will increase significantly due to the obstruction of satellite signals. To address the challenges, researchers have discussed the application of multiple technologies for indoor positioning, such as WiFi [38, 43, 74, 80], Bluetooth [92], mmWave [61], **radiofrequency identification (RFID)** [21, 34, 53, 75], UWB [23, 64, 68, 73], acoustic signals [26, 50, 87, 90], and visible light [44, 47, 54, 79]. Among them, UWB is considered to be one of the promising technologies for high-precision indoor positioning due to its low energy consumption, centimeter-level positioning

Table 1. Comparison of Different Indoor Positioning Technologies

Technology	Maximum working distance	Positioning accuracy	Power consumption
WiFi	35 m	~5 m	Moderate
Bluetooth	50 m	~5 m	Low
mmWave	200 m	0.2-0.5 m	High
RFID	200 m	~5 m	Low
Acoustic	< 10 m	0.1-0.5 m	Low
Visible light	200 m (LOS)	0.1-0.5 m	High
UWB	15-50 m	2-50 cm	Moderate

resolution, and multipath resistance. Similar to methods in [23, 83], we compare the maximum working distance, positioning accuracy, and power consumption of these technologies in Table 1.

UWB technology transmits ultra-short nanosecond-level pulse signals over a very large frequency band and can use short duty cycles, thereby reducing system power consumption. The high bandwidth of UWB technology allows it to achieve high-precision positioning. This precision is particularly valuable in applications in which precise location tracking is critical, such as asset tracking in warehouses, indoor navigation in complex environments, and augmented reality.

2.2 UWB Ranging

In wireless networks, CIR is a good description of the attenuation and delay of the received signal through the wireless channel. Suppose that there are L paths, and the signal from path i has a delay τ_i and amplitude α_i. The CIR can be represented as [69]

$$h(t) = \sum_{i=1}^{L} \alpha_i e^{-j2\pi f_c \tau_i} \delta(t - \tau_i), \tag{1}$$

where $\delta(t - \tau_i)$ is Dirac's delta function [8].

For high-precision timestamp estimation, a UWB chip first records the CIR with a resolution of a nanosecond upon receiving packets. Then, it uses some dedicated algorithms (e.g., **the Linear Discriminant Analysis (LDE)** algorithm [6]) to find the first path from CIR and calculate the corresponding arriving timestamp. An example of a CIR is shown in Figure 2(a). We can find the first path as the first sharp peak, thus deriving the corresponding timestamp.

With the timestamp, IEEE 802.15.4 [31] recommends a **two-way ranging (TWR)** method for UWB ranging. Figure 1 shows two kinds of TWR methods: the **single-sided TWR (SS-TWR)** and the **double-sided TWR (DS-TWR)** [37]. SS-TWR takes one packet back and forth between a tag and an anchor (e.g., A_1). The **Time-of-Flight (TOF)** is calculated as

$$T_f = \frac{1}{2}((t_{TR1} - t_{TP}) - (t_{A1R1} - t_{A1P})). \tag{2}$$

The DS-TWR algorithm [37] adds an extra packet exchange based on SS-TWR for more accurate ranging, forming $Poll - Resp - Final$ packet exchanges. The TOF thus can be calculated as [58]

$$T_f = \frac{(t_{TR1} - t_{TP})(t_{A1F} - t_{A1R1}) - (t_{TF} - t_{TR2})(t_{A1R1} - t_{A1P})}{(t_{TF} - t_{TP}) + (t_{A1F} - t_{A1P})}. \tag{3}$$

2.3 The Impact of NLOS

We conduct experiments in the laboratory setting to demonstrate the influence of NLOS scenarios on UWB ranging and positioning. In Figure 11, we place an anchor at a fixed position while volunteers stand at various positions holding a UWB tag. Our primary focus is on investigating signal

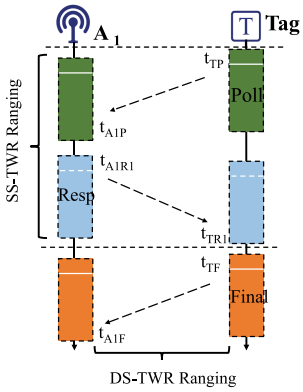

Fig. 1. The two-way ranging (TWR) algorithm.

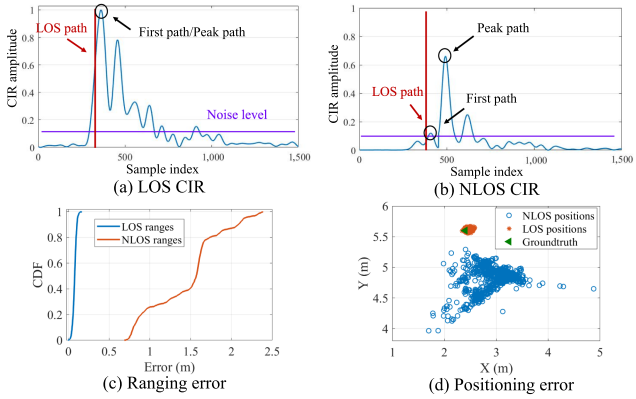

Fig. 2. (a) and (b) show the channel impulse response (CIR) in LOS and NLOS, whereas (c) and (d) show the ranging and positioning error in LOS and NLOS.

obstruction caused by the human body, a commonly encountered scenario. We plot the CIR of both LOS and NLOS links in Figures 2(a) and 2(b). For LOS links, we can observe a sharp peak for the first path, thus obtaining the accurate timestamp. However, for NLOS links, the first path experiences attenuation, falling even below the noise threshold, leading to inaccuracies in estimating the first path and timestamps.

We further examine the impact of NLOS on ranging and positioning. In Figure 2(c), it is evident that in LOS scenarios, we can achieve an approximate ranging error of nearly 10 cm. However, in NLOS scenarios, the ranging error swiftly escalates to more than 2 m. Additionally, Figure 2(d) illustrates that the measured position closely aligns with the true position in LOS scenarios. Conversely, in NLOS scenarios, the resulting positions exhibit significant variation, with errors extending to several meters.

2.4 Observations

Three observations motivate our design.

Observation 1. *The identification task for anchor links is much easier than that of tag links.*

For ranging systems, NLOS conditions directly affect the accuracy of distance measurements. Therefore, the most intuitive method is to identify the link status based on the magnitude of ranging errors. Greater ranging errors typically signify a higher likelihood of an NLOS link. This method is not feasible for tags since their positions are unknown. However, it can be effectively applied to anchors due to their known locations. Leveraging the known positions of anchors enables straightforward identification of their respective links.

Observation 2. *Even though NLOS links can vary significantly in the same environment, LOS links possess very similar features no matter what position in UWB.*

The variation of NLOS links is comprehensible due to the potential alteration of ranging outcomes caused by diverse obstacles and varying distances to these obstacles.

One of the advantageous characteristics of UWB technology is its high tolerance for multipath interference. Essentially, UWB demonstrates accurate ranging outcomes regardless of the device's position within an environment, as long as an LOS condition is maintained. We thus conduct a comparison of ranging performance in four distinct settings: Weak multipath by putting devices on the top of poles, strong multipath by putting devices near the wall, strong multipath by putting devices on the ground,

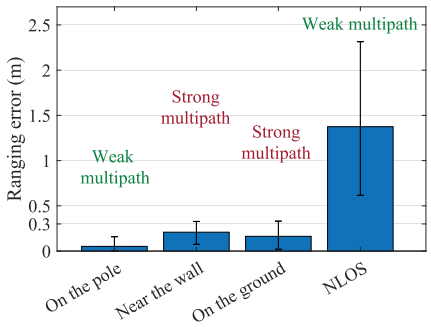

Fig. 3. Ranging errors in case of weak multipath (LOS), strong multipath (LOS), and NLOS conditions.

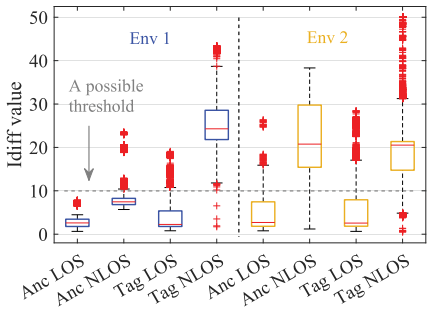

Fig. 4. Anchor link and tag link comparison in two scenes by the channel feature $Idiff$.

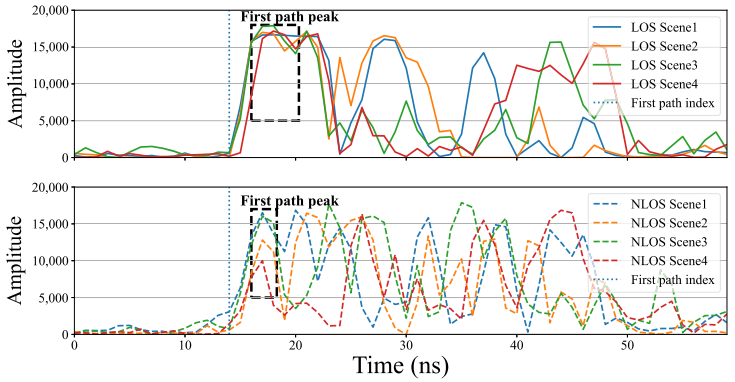

Fig. 5. CIR of LOS and NLOS links collected by commercial DW1000 chips at different positions in the same room.

and weak multipath in NLOS by manually blocking devices. The findings in Figure 3 display that for LOS, even under strong multipath conditions, the ranging error remains below 0.3 m. However, in NLOS scenarios, the mean error rapidly elevates to 1.23 m. Further, we fix an anchor and put the tag at different positions within our laboratory to collect CIR data for different LOS and NLOS links, as depicted in Figure 5. The upper section illustrates four LOS links, while the bottom section displays four NLOS links. The dashed black box outlines the estimated first path in the figure. In LOS links, a distinct first path is evident, leading to high similarity among them for two key reasons. First, the first path in LOS conditions typically follows the shortest route, accumulating substantial power at the receiver within the entire CIR [6]. Second, UWB technology can effectively separate the first path and other paths in LOS conditions, leading to accurate first-path estimation even in rich-multipath environments. Conversely, for NLOS links, we observe that the first path is much weaker and is usually not the highest one. Thus, it is more susceptible to noise and is challenging to estimate. In summary, UWB LOS links exhibit similar features whereas NLOS links can vary significantly within the same environment.

Observation 3. *Anchor LOS links present similar features to tag LOS links.*

Currently, the hardware for UWB devices, both in anchors and tags, is nearly identical, differing mainly in power consumption. Therefore, we can reasonably infer that there is no essential difference between the anchor–anchor LOS link and the anchor–tag LOS link. Thus, we propose utilizing LOS links among anchors to assist in identifying tag links. To demonstrate the feasibility, we categorize UWB links into four groups: LOS and NLOS links between anchors (Anc LOS, Anc NLOS), and LOS

and NLOS links between tags and anchors (Tag LOS, Tag NLOS). We employ a widely used channel feature called $Idiff$ [5] to characterize link statuses. $Idiff$ is calculated as the difference between the index of the peak path and the first path in the CIR. In an LOS link, $Idiff$ tends to approach 0, as showcased in Figure 2(a), since the peak path typically aligns closely with the first path. Conversely, in an NLOS link, $Idiff$ tends to be larger because the first path usually differs significantly from the peak path.

Figure 4 shows the result in two different environments. Notably, $Idiff$ values are small for both Anc LOS and Tag LOS links, whereas they are large for both Anc NLOS and Tag NLOS links. This observation supports our expectation that $Idiff$ values for anchor LOS links strongly resemble those of tag LOS links within the same environment. Moreover, attempting to differentiate LOS and NLOS links using a predefined threshold appears effective in Env 2 but fails in Env 1. This outcome emphasizes the challenge of employing a universal threshold across different environments. The findings demonstrate the feasibility of using LOS anchor links to identify LOS tag links based on similarity, thus achieving the objective of tag link identification.

2.5 The Advance of Our Method

Our method of leveraging anchor links to assist link identification has two major advantages.

(1) Our method can adapt to different environments. The adaptability of our method across various environments becomes evident when comparing two contrasting settings: an indoor laboratory and an outdoor parking lot. The laboratory setting, with its numerous obstacles, exhibits rich multipath characteristics, whereas the parking lot represents an open space with superior link quality and minimal obstructions. As a result, the utilization of a single threshold for distinguishing mixed links between these two environments becomes challenging, leading to issues in environmental adaptability. However, our proposed method offers a solution by identifying link statuses based on anchor links within their specific environments. This adaptability stems from leveraging anchor links as a reference point to discern link statuses, allowing the approach to accommodate variations across different environments.

(2) Our method requires no prior data collection and training, incurring little overhead. Our method manages to obtain real-time anchor link information and use it for tag link identification. Notably, it eliminates the necessity of collecting prior data for system calibration or training, thus minimizing overhead. Simultaneously, we endeavor to circumvent additional system overhead, such as identifying anchor link status without requiring extra ranging messages, and mitigating NLOS errors using fast-converging algorithms. This approach aims to maintain efficiency while achieving accurate tag link identification without burdening the system with unnecessary additional processes.

3 REFLOC DESIGN

Figure 6 illustrates the main design of RefLoc, comprising four components: Anchor Link Identification, Feature Extraction, Tag Link Identification, and NLOS–based Localization. We first manage to infer the link status of anchors with low cost in the Anchor Link Identification component. Then, we estimate the quality of features in terms of link identification, select the most effective ones, and infer their confidence factors in the Feature Extraction component. Based on referenced anchor links and selected features, we can identify tag links and finally mitigate the NLOS effect on localization in the third and fourth components separately.

3.1 Anchor Link Identification

This component has two goals: (1) collect channel information among anchors and (2) classify the link status of anchor links.

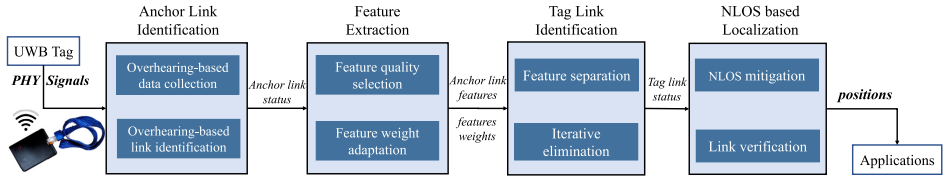

Fig. 6. The system framework for RefLoc.

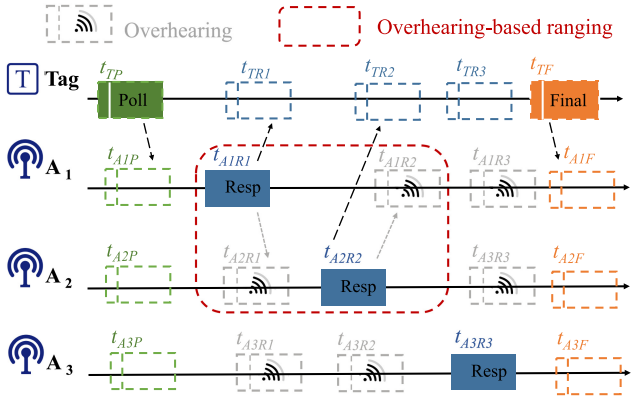

Fig. 7. Overhearing-based data collection and ranging for anchors.

3.1.1 Overhearing-Based Data Collection. Intuitively, we can let each anchor actively transmit packets for data collection. However, this approach brings in extra overhead and delays. Considering that current ranging systems already have large messages overhead and high system costs, adopting such methods might prove unacceptable. We instead achieve the goal by employing overhearing during the tag ranging process. We illustrate the process in Figure 7, where the tag employs the DS-TWR method for ranging. During the tag-anchor communication, each anchor can overhear *Resp* packets from other anchors. For example, A_2 can overhear the *Resp* packet from A_1 and estimate the CIR of the link. Similarly, A_1 can also overhear packets from A_2 and estimate the corresponding CIR. The entire process occurs during the tag ranging process without additional overhead. The information can be updated whenever a tag performs ranging.

3.1.2 Anchor Link Identification. Upon obtaining the channel information among anchors, the subsequent step involves classifying these anchor links. Note that the status of anchor links may fluctuate across diverse environments and timeframes. Factors such as a person's movement or rearrangement of furniture can transform an LOS anchor link into an NLOS link, or conversely, transform an NLOS link back into an LOS link.

We exploit that the position of anchors is often known in advance [9, 17, 76] and design a ranging-based identification method. The red dotted frame in Figure 7 illustrates the anchor ranging process. By overhearing, the two anchors can receive *Resp* packets from each other and timestamp the packets (i.e., t_{A2R1} and t_{A1R2}). The two overhearing packets along with the raw two *Resp* packets (i.e., t_{A1R1} and t_{A2R2}) can form an SS-TWR process. Therefore, the range is calculated as $T_f = \frac{1}{2}((t_{A1R2} - t_{A1R1}) - (t_{A2R2} - t_{A2R1}))$. Nevertheless, as noted in [58, 72], the SS-TWR method is error prone due to the extended response interval of $(t_{A2R2} - t_{A2R1})$. To address the problem, we propose two solutions. The first is to accurately schedule anchors so that the interval is as short as possible. The second is to leverage more anchors to improve the ranging accuracy. Considering that there is another anchor A_3, we can use one anchor for time synchronization, thus greatly im-

Table 2. Candidate Feature List

Name	Equation
Energy	$\epsilon = \sum_1^T r(t)^2$
Maximum amplitude	$r_{max} = \max\|r(t)\|$
Kurtosis	$\mu = \frac{1}{T}\sum_1^T r(t)\ \sigma^2 = \frac{1}{T}\sum_1^T \|r(t)-\mu\|^2$ $k = \sigma^4 T \sum_1^T \|r(t)-\mu\|^4$
Mean excess delay	$\tau_{MED} = \sum_1^T t\frac{r(t)^2}{\epsilon}$
RMS delay spread	$\sum_1^T (t-\tau_{MED})^2 \frac{r(t)^2}{\epsilon}$
Rise time	$t_{rise} = t_H - t_L\ t_L = FP\_ind$ $t_H = \min t : \|r(t)\| \geq 0.6 * r_{max}$
Mc	$r_{FP\_ind} - r_{max}$
Idiff	$\|FP\_ind - Peak\_ind\|\ r(Peak\_ind) = r_{max}$
Pw	$\epsilon - FP\_pw$
The standard Noise	Estimated by UWB chips

$r(t)$ is the estimated CIR data and T is its length.

proving the SS-TWR ranging accuracy between the other anchors. The method is feasible due to the known positions of anchors and also requires no additional process between anchors.

For NLOS links, the estimated range r significantly deviates from the ideal range $\widehat{r}$ due to incorrect timestamps. Therefore, we can identify the link by the ranging error $e = |r - \widehat{r}|$. We set a link as an NLOS link when the ranging error is large (e.g., $e \geq thr$). Otherwise, we set the link as an LOS link. Note that thr is determined by the deviation between estimated ranges and ideal ranges that are relatively independent of environments, taking into account the anti-multipath characteristics of UWB. Empirically, we set thr at 0.3 m, as validated through experiments detailed in Section 2.4.

3.2 Feature Extraction

Rather than utilizing the CIR directly, we extract channel features from it based on which we can identify links with small amounts of data. Typically, numerous channel features can be extracted, such as amplitude, **Root Mean Square (RMS)** delay, and signal energy, among others [14, 65, 66]. However, not all extracted features prove effective or useful for identifying UWB links. Therefore, the crucial question arises: how do we assess the importance of these features and amalgamate the most significant ones for accurate link identification?

Numerous studies have delved into feature selection to enhance link identification [25, 86]. However, they usually select an optimal set of features and give their equal weights. We instead want to select effective features and rank them for better feature fusion. To address the problem, we adopt a widely used feature selection method: the **Chi-Square (CS)** test [1]. To perform the CS test, we first collect a total of 10 commonly used features from both LOS and NLOS links. As listed in Table 2, all features can be inferred from CIR data $r(t)$ of length T. Then, we use a **Support Vector Machine (SVM)** for link classification. For feature i, we can obtain two data clusters by the SVM, and calculate its confusion matrix with four metrics: **True Positive (TP_i)**, **True Negative (TN_i)**, **False Positive (FP_i)**, and **False Negative (FN_i)**. The quality of the feature is calculated as

$$\chi^2(i) = \frac{TP_i \times TN_i - FN_i \times FP_i}{(TP_i + FN_i)(FP_i + TN_i)}, \tag{4}$$

where $\chi^2(i)$ indicates the quality of feature i. For a good feature, the FN and FP should equal 0; thus $\chi^2(i)$ should be close to 1.

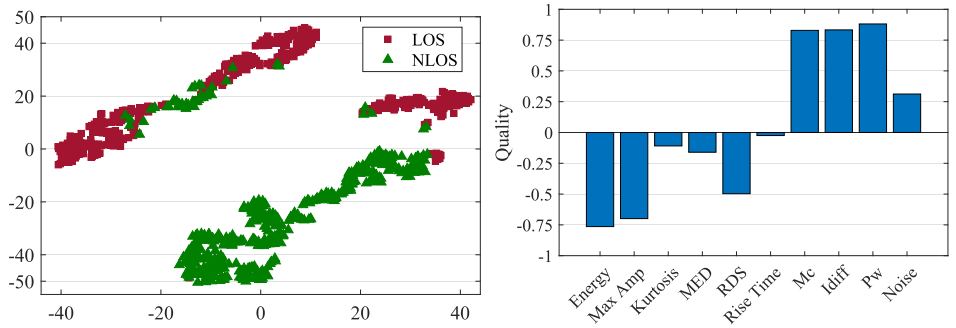

(a) Classification result by SVM based on Pw (b) Quality of features

Fig. 8. Feature selection by the Chi-Square test. (a) shows an example of clustering result. (b) shows the quality of different features (1: best, -1: worst).

We show a classification result of SVM by the feature Pw in Figure 8(a). As seen in Table 2, Pw is the difference between the signal energy and the first path energy. We see that Pw is a good feature, as it can separate two types of links. Then, we can calculate the feature quality by Equation (4). In this way, we calculate all feature quality and show the result in Figure 8(b). We see that the quality of Mc, $Idiff$, Pw, and *the standard noise* are high whereas others are low. We can easily infer that those features highly related to multipath tend to have poor quality, as UWB is relatively resilient to multipath. The four features, however, are weakly correlated with multipath but strongly correlated with the first path, thus, have good quality as analyzed in Section 2.4.

Based on the results, we choose four indicators, i.e., Mc, $Idiff$, Pw, and *the standard noise*, to capture the link feature and use them for subsequent tag link identification. The calculated feature quality can also be used as a confidence factor for each feature, which helps us perform better multi-feature fusion for link identification.

3.3 Tag Link Identification

We now can leverage the inferred anchor links and extracted features to identify tag links.

3.3.1 Feature Separation. As shown in Figure 9(a), we can cluster features of both tag and anchor links into two categories: $Group1$, containing anchor LOS links, and $Group2$, containing anchor NLOS links. Tag links are all marked by black circles. We see that $link$-1 is an LOS link since it is in $Group1$. The other tag links are NLOS links, as they are in $Group2$.

However, two problems prevent us from making robust clustering. The first problem is the extremely small amount of data, e.g., there are only three packets (i.e., three CIRs) for link identification in a single DS-TWR process. Thus, it is easy to misidentify the links. As shown in Figure 9(b), $link$-2 is misjudged since most of its data falls into $Group1$ due to outliers even though it is a NLOS link. The second problem is the large deviations of NLOS features. The deviations of NLOS features are various with obstacles and distances, leading to wrong clustering results. Figure 9(c) shows that $Group2$ only contains $link$-2 due to its large deviation. As a result, other NLOS links are misjudged.

3.3.2 Iterative Elimination. To solve these problems, we leverage an iterative elimination method based on multi-dimensional information fusion. Specifically, given N consecutive measurements, we can obtain a total of $3N$ data for link identification. Figure 9(d) shows a clustering result of three consecutive measurements. We can divide $link$-3 into the LOS status since most of its data belong to $Group2$. We see that consecutive measurements make the result more resilient to outliers. We set $N = 5$ empirically with a time cost of less than 100 ms.

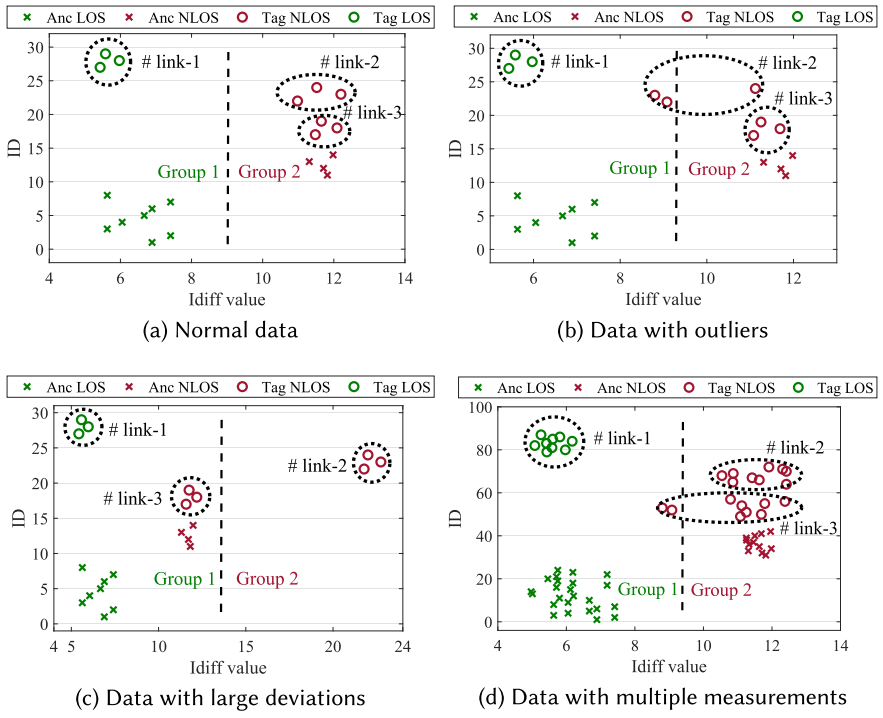

(a) Normal data (b) Data with outliers

(c) Data with large deviations (d) Data with multiple measurements

Fig. 9. Clustering results of (a) normal data, (b) data with large deviations, (c) data with outliers, and (d) data with multiple measurements. The black circles mark different tag links.

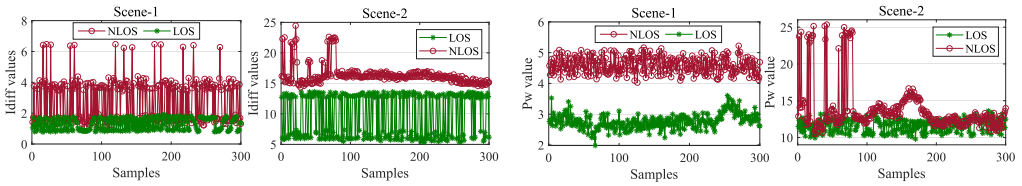

(a) $Idiff$ of two links is partially confused in scene-1, while is separated clearly in scene-2.

(b) Pw of both links is separated apparently in scene-1, and is partially confused in scene-2.

Fig. 10. Link measurement with two features in different scenes. It shows that the distinguishing ability of features can be different in different scenarios.

We further leverage multiple features to enhance the result. Suppose that there are m tag links; for the j^{th} feature, we can obtain an identification result $R_j = (r_1, r_2, \ldots, r_m)$, where $r_i = 0$ *or* 1 $(i = 1, 2, \ldots, m)$ indicates whether the i^{th} link is an NLOS link. We can calculate a combined identification result of R by

$$R = \frac{\sum W_j \cdot R_j}{\sum W_j}, \tag{5}$$

where W_j is the weight for the j^{th} feature. When R is close to 1, the link tends to be an NLOS link and vice versa. The weight W_j should also be carefully designed as the performance of features can vary depending on the environment. For example, Figure 10 shows link measurements in two scenes with $Idiff$ and Pw features. We see that the $Idiff$ of two links mix partially in scene-1

whereas they are separated clearly in scene-2. In contrast, Pw of both links are well separated in scene-1 and become partially confused in scene-2. The result indicates that we need to adaptively combine different features to obtain accurate results. Therefore, we first normalize values of all features to a range of $[0, 1]$. Given LOS links of the j^{th} feature as los_j and NLOS links as $nlos_j$, we infer its weight as $W_j = \frac{|\sum_1^N (los_j - nlos_j)|}{N} \cdot Qua_j$, where N is the number of samples and Qua_j is the quality of the j^{th} feature inferred in Section 3.2.

After obtaining R, we then iteratively filter out the NLOS links instead of directly identifying all links to resolve the problem of large deviations. Take Figure 9(c), for example. We can first confirm $link$-2 as the NLOS link whose value is mostly close to 1, thus filtering it out. Then, we repeat the process and iteratively find $link$-3 and anchor NLOS links.

3.4 NLOS-Based Localization

We first adopt the TS-based LS algorithm to mitigate the impact of NLOS links and then design a link verification method to validate results and deal with misidentifications. In this section, although the TL-LS algorithm is an existing mature algorithm, our main contribution is to use the link confidences we defined as the algorithm input and to identify and fix the errors that occur when tracking moving tags.

3.4.1 The TL-LS Algorithm. Though there are several NLOS mitigation algorithms, we choose the TL-LS algorithm due to its efficiency and low computation cost [18, 81]. We compare the algorithm with other methods in our evaluation (Section 4.3.2) and show its superiority in terms of the trade-off between both ranging accuracy and computation cost.

The TL-LS algorithm is similar to the trilateration positioning algorithm based on least squares optimization, but it assigns different weights to the LOS and NLOS ranging values and updates the positioning results in iterations. The key working principle of the algorithm is that the LOS ranges involved in the position calculation can suppress the NLOS effect; the updated ranges for NLOS links are more accurate than the original NLOS ranges [81]. Therefore, we can replace the original NLOS ranges with the new ones and iteratively obtain more accurate positions. We set the diagonal weight matrix of the TL-LS algorithm as $diag(1 - R)$, where R is the identification result for link status calculated by Equation (5). The positioning results will be refined iteratively until the convergence threshold is reached or the iteration limit is reached.

3.4.2 Link Verification. We may obtain incorrect link identification results owing to complex environments and imperfect hardware, which, in turn, causes large positioning errors. We thus propose a link verification method to cope with misidentifications. Whenever the estimated position by RefLoc is detected as an outlier, for example, if the position is far away (e.g., $0.5\,m$) from the last position, we assume that the position is wrong and take the last position as the hypothetical position. With the hypothetical position, we can calculate an assumed ideal range ($\widehat{r}$). Then, we can use the ranging-based identification method in Section 3.1.2 to re-identify links. Thus we can again perform NLOS mitigation based on the new identification result and get the refined position. The premise of such a method is that the moving distance between adjacent sampling points is small, which is a reasonable assumption in many applications.

4 IMPLEMENTATION AND EVALUATION

We implement RefLoc with commercial UWB hardware shown in Figure 11. The hardware comprises a DW1000 chip, an STM32F103T8 MCU, and an antenna having a gain of 5 dBi. Our configuration for DW1000 involves setting a bandwidth of 499.2 MHz, a carrier frequency of 3993.6 MHz, a data rate of 110 kbps, and a **pulse repetition frequency (PRF)** of 16 MHz. Additionally,

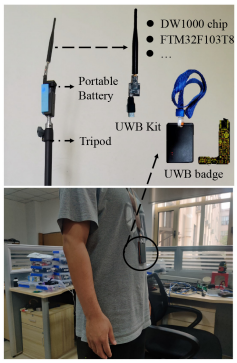

Fig. 11. Commercial UWB hardware used in our experiments. We also build a UWB badge.

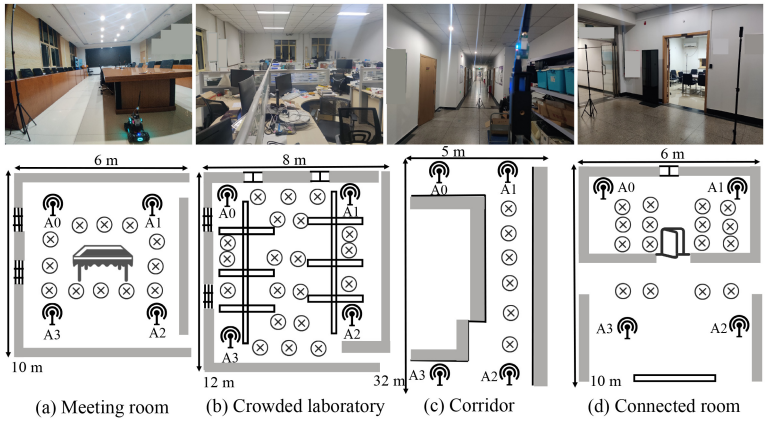

Fig. 12. Various indoor experiment environments. The circled crosses are the tested positions.

we build a UWB-embedded badge intended for tracking individuals, as displayed on the right side of the figure.

4.1 Experiment Setup

As shown in Figure 12, we evaluate RefLoc within four distinct indoor environments:

(a) *Meeting room (m-room).* The room is about 6 m × 10 m with few pieces of furniture.
(b) *Crowded Laboratory (lab).* This is a laboratory of 8 m × 12 m. The laboratory is furnished with tables, chairs, and laboratory apparatus, among other items.
(c) *Corridor.* The area of the corridor is about 5 m × 35 m. There is a wall to block both tag and anchor signals.
(d) *Connected room (c-room).* The area is 6 m × 10 m. It is a small room connected to the corridor. There is a door to block UWB signals.

In each environment, we instruct volunteers to wear the badge and stand at various positions indicated by circled forks in Figure 12. Our observations reveal that the presence of the human body obstructs the UWB connection to a minimum of two anchors across these environments. Consequently, despite deploying four anchors, the number of LOS links remains consistently below three.

4.2 Identification Performance

We collect data at each position three times in different environments. At each position, we run methods for at least 5 minutes. We show the average identification accuracy of both LOS and NLOS links if not specified.

4.2.1 Overall Performance. The performance of RefLoc in four environments is shown in Figure 13(a). We see that the identification accuracy is above 96% for tag links and nearly 100% for anchor links in all environments. The high identification accuracy of anchor links provides good references for tag link identification. The result indicates that our method can effectively distinguish both LOS and NLOS links. More importantly, it can adapt to various indoor environments. However, it is strange to see that the worst identification accuracy appears in the meeting

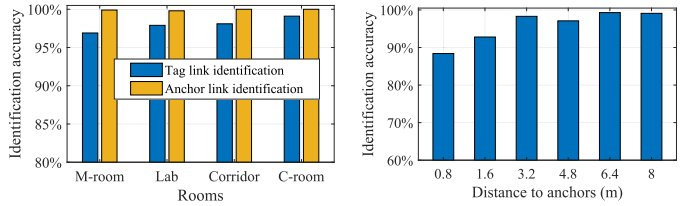

(a) Identification in four environments

(b) Identification with different distances

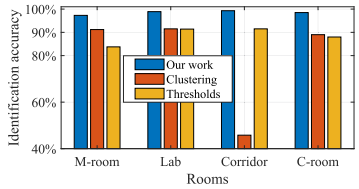

(c) Identification comparison

Fig. 13. Identification results in the case of different environments, distances, and methods.

room with few obstacles. We think that the rich multipath in complex environments would make NLOS links worse, making it easier to identify the NLOS links from LOS links. Therefore, the identification accuracy in the other three environments is better than that in the meeting room.

4.2.2 Impact of Distance. We then investigate the impact of distance on link identifications in the meeting room. We let the volunteers stand at different distances to anchor A_0 with their backs to the anchor. Therefore, the link from the badge to A_0 is always blocked. We collect data and show the identification accuracy in Figure 13(a). We see that as the distance increases, the accuracy of NLOS identification also increases. The identification accuracy is above 92% when the distance exceeds 1.6 m. However, the accuracy decreases to about 88% when the distance is small (e.g., only 0.8 m from the anchor). The reason is that when the distance is small, the blocked received signal may still be strong and comparable to LOS signals, causing decreases in identification accuracy.

4.2.3 Comparison of Different Methods. We compare RefLoc with two common link identification methods.

(a) *Threshold*: We extract features from the CIR and adopt a predefined threshold for link identification. We use the most popular *Pw* feature for identification [84]. We set thresholds in the lab and use them for other environments.
(b) *Clustering*: We extract features from the CIR and cluster features without referenced anchor links.

Figure 13(c) shows the results. The *Clustering* method obtains around 90% accuracy in most environments, yet has very low accuracy in the corridor. Since links in the corridor vary significantly due to blockage of the wall and the human body, the *Clustering* method fails to cope with such a large bias between links. The *Threshold* method achieves a good accuracy of above 90% in the lab and the corridor. However, the accuracy falls below 85% in the meeting room. Thus, the two methods cannot adapt to different environments well. RefLoc achieves an identification accuracy of above 96% in all environments, improving accuracy around an average of 10% compared with the *Threshold* method.

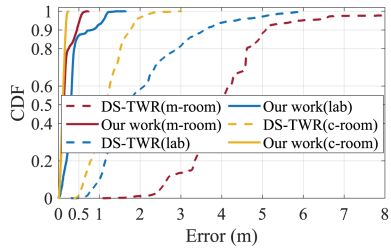

(a) Positioning error in the meeting room(m-room), the connected room (c-room), and the laboratory(lab).

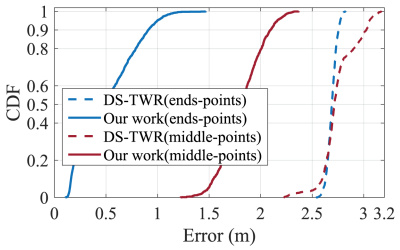

(b) Positioning error of ends-points and middle-points in the long Corridor.

Fig. 14. Localization performance of RefLoc in different environments.

4.3 Localization Performance

4.3.1 Performance in Different Environments. Figure 14 shows the localization performance. The left figure shows the **cumulative distribution function (CDF)** of average positioning error in three environments. We see that for the DS-TWR method, the median and 90% localization error of the meeting room, the connected room, and the lab are (4.10 m, 5.07 m), (0.51 m, 1.76 m), and (1.60 m, 2.41 m). The result indicates that NLOS links can incur very large errors for UWB localization. With RefLoc, however, the median and 90% error become (0.17 m, 0.41 m), (0.102 m, 0.18 m), and (0.31 m, 0.42 m) for the three environments, reducing the 90% error by 91.9%, 89.7%, and 82.6%, respectively. We note that the largest position error of DS-TWR is in the meeting room with few obstacles. The reason is that in that room, the ranging errors of NLOS links are the largest whereas, in other environments, there is likely a path arriving faster than the attenuated LOS signal, resulting in slightly better ranging results.

Since there is only one LOS link when volunteers wearing the badge stand in the corridor, the TL-LS method fails in this situation. We thus place the device on a tripod for localization. Figure 14(b) demonstrates the result. We divide the positions (Figure 12(c)) into the end-points and the middle-points. We see that the median error of DS-TWR is about 2.69 m and 2.71 m for end-points and middle-points, and becomes 0.47 m and 1.82 m in our work. Such a result is much larger than those in the other three environments. The reason is that the long-ranging distance in the corridor brings significant position errors even with two LOS links of small ranging errors. That is also why the middle-points incur more position errors than the end-points.

4.3.2 Effectiveness of NLOS Mitigation. In order to verify that the TL-LS algorithm used by RefLoc has better effectiveness in NLOS mitigation, we compare our work with four localization methods in terms of positioning error and time cost in the lab.

(a) *DS-TWR*: A standard ranging method that complies with the 802.15.4 [31], and the ranging values of LOS and NLOS links will be directly used for trilateration positioning. This method does not deal with the NLOS problem.
(b) *Base-Cali*: A straightforward method that uses two LOS links and a randomly chosen NLOS link for trilateration positioning.
(c) *Fusic*: A state-of-the-art NLOS mitigation algorithm by correction of ranging values under NLOS conditions by using CIR [39].
(d) *LP (Linear Programming)*: A widely used NLOS mitigation method that uses the idea of linear programming to solve the position [70]. This method relies on the classification results of LOS and NLOS links.

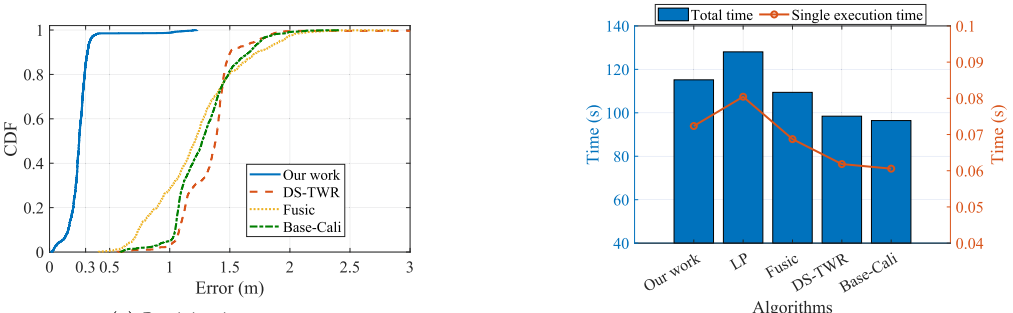

(a) Positioning error

(b) Time cost

Fig. 15. Localization comparison of different methods. (a) Positioning error. (b) Time cost.

The results of method (a) and method (b) can be regarded as baseline references.

Positioning error. Figure 15(a) shows the CDF of positioning error. We see that the median error of DS-TWR is 1.38 m, which is the worst result as it does not eliminate NLOS. *Base-Cali* is slightly better than *DS-TWR*, with a median error of 1.28 m by discarding one NLOS link. *Fusic* tries to find the actual first path affected by NLOS and has a median error of 1.21 m, since it cannot eliminate the time delay caused by occlusions, e.g., the time delay traveling through the human body. RefLoc achieves a median error of 0.31 m, which is significantly better than the other work. Note that we do not show the *LP* method here, as it fails to work with less than 3 LOS links.

Time cost. We show the total time and the average single execution time of each method in Figure 15(b). The *DS-TWR* method provides a baseline as it does not use any mitigation methods. The *Base-Cali* method simply ignores one link, thus having the lowest time cost. The *Fusic* method is a one-step method that directly corrects the NLOS results, costing a moderate amount of time. In contrast, the *LP* method takes the longest time due to large computations. Our system costs about 75 *ms* for a single execution, facilitating around a 10% reduction of overhead compared with the *LP* method while taking more time than others due to multiple iterations.

In summary, RefLoc can achieve a significant ranging improvement at the cost of a small amount of time overhead.

4.4 Tracking with RefLoc

We build an application for real-time people tracking in the lab. The detailed deployment is shown in Figure 16(b). We mark four anchors with red circles. For ease of testing, we ask the volunteer to walk around the room along a predefined trajectory (a green line in the figure) at his usual speed.

The tracking result is shown in Figure 16(a). The black dotted line is the actual movement trajectory of the volunteer. The blue dots are the tracking result of DS-TWR, and the orange dots are the result of RefLoc. We see that the tracking results are unpredictable and irregular for DS-TWR due to the impact of NLOS. However, the trajectory of RefLoc is very close to the actual one, with a positioning error of most points less than 0.5 m.

We further show the ranging error and link variations of both a tag link and an anchor link during the tracking in Figure 17. We see a strong correlation between the feature variations and the ranging error of the tag link, as they become messy or clear at nearly the same time. During the entire process, the link feature of anchors remains constant due to the LOS condition. We see the strong similarity of features (i.e., similar values) between tag LOS links and anchor LOS links, which again shows the feasibility of our work.

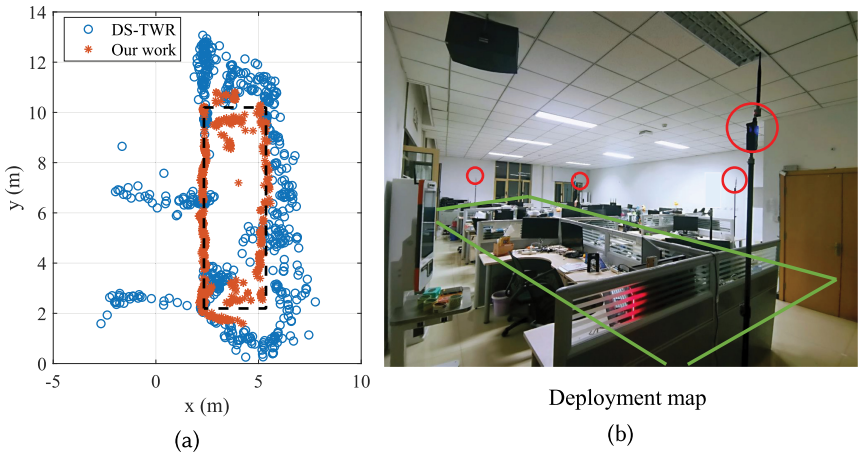

Fig. 16. Real-time tracking by RefLoc. (a) the trajectory. (b) the deployment map, where the red circles mark the anchor locations and the green line is the ground-truth.

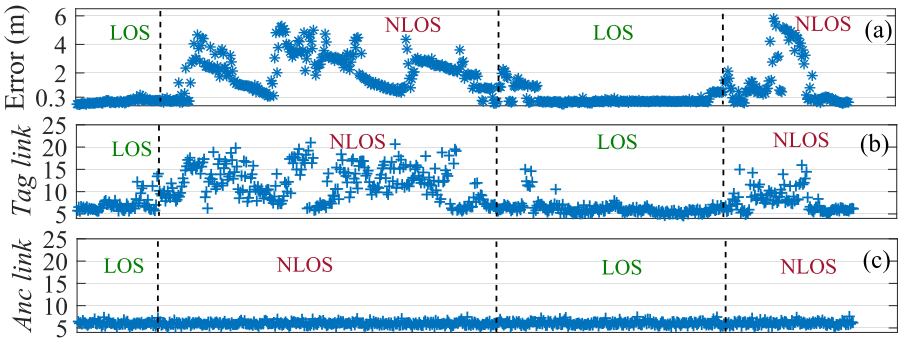

Fig. 17. Link variations during the tracking. (a) The ranging error of the tag link. (b) and (c) show the variations of the Pw feature for both the tag and anchor link.

5 RELATED WORKS

The NLOS issue has been studied in the literature for years, and plenty of NLOS identification and mitigation techniques have emerged accordingly. We introduce related works from the two aspects and mainly focus on those works related to UWB technology.

NLOS identification: To facilitate comparison with our work, we divide this type of work into two categories: the prior-knowledge-based solution and the one-step solution.

The prior knowledge-based solution also includes two methods: the first is the statistics-based method, and the second is the machine learning method. The statistics-based method collects data from different links, analyzes and infers the data distribution characteristics, and then performs link status identification [13, 20, 22, 33, 49, 57, 78, 82, 85, 89, 91]. For instance, [20] collects data to infer multi-modal noise distributions to characterize NLOS results whereas [22] performs data processing in advance to obtain the distribution of ranging results of different links and uses it for link identification. These methods typically require extensive data collection and measurements to infer statistical characteristics, causing high overhead and labor costs. Note that the statistical characteristic drawn from one scenario may not apply to another scenario, causing the problem of environmental adaptability. The machine learning method is completely

data driven, relying on a large amount of data, label preprocessing, and then learning and training [12, 25, 36, 48, 51, 52, 60, 62, 65, 67, 77, 86]. These methods focus on feature extraction and neural network design. The work in [86] tries different tenants with 18 features to achieve better link identification, and the work in [25] not only tries different feature combinations but also utilizes various machine learning algorithms. Such methods work well if trained well. But its shortcomings are also obvious, that is, it requires a large amount of data to train and it is usually applicable to a specific environment.

The one-step solution aims to achieve fast and effective link identification. It tries to find key indicators and adopts empirical parameters for link identification in a few measurements [5, 10, 11, 24, 32, 42, 46]. For example, the work in both [42] and [32] use the *Pw* feature calculated from CIR data and use a simple threshold for link identification. The work in [5] proposes several indicators and uses them for link identification in order. These methods, however, may fail to adapt to different environments and hardware.

This article proposes to leverage referenced anchor links to assist tag link identification with no prior data collection and training. Our method is adapted to various environments due to real-time anchor link information in respective environments. Therefore, our approach is lightweight and capable of plug-and-play applications.

NLOS mitigation: The first method is based on filtering algorithms, e.g., the Kalman filter [45]. The algorithm smooths and corrects NLOS results through trajectory analysis and motion modeling. The second is based on dedicated NLOS mitigation algorithms [63, 71], including RWGH [15], TL-LS [18], and more. The core of the algorithms is to correct NLOS ranges based on geometric constraints with LOS ranges. Nevertheless, most of those algorithms require heavy computations and multiple LOS anchors. Another widely used method is machine learning [48, 65], which is employed to analyze sets of real results captured in various scenarios for NLOS mitigation. The method works effectively but requires laborious data collection and can be too heavy to run on low-cost **Internet of Things (IoT)** platforms. The core contribution of RefLoc focuses on link identification. We derive link confidences and fit them into the TL-LS algorithm to implement a low-cost localization system.

6 LIMITATION AND FUTURE WORK

Though we have evaluated the feasibility and efficiency of RefLoc, there are indeed limitations and future work to further improve the system.

(1) RefLoc relies on the existence of anchor LOS links. As we have explained, LOS links have similar features whereas NLOS links are various. Therefore, in principle, only the LOS link serves as a reference for other links. Even so, we believe that anchor LOS links exist with a high probability in practical application scenarios, considering that anchors are typically well deployed.

(2) RefLoc mainly verifies the NLOS scene of human body occlusion; on this basis, the system is implemented and applied. Honestly speaking, the purpose of this article is to address the NLOS challenge within human positioning and tracking, aiming to design and implement a practical human localization system. For future work, we intend to delve into exploring more intricate and diverse NLOS scenarios.

(3) We can improve the performance of RefLoc with many mature and robust technologies. As introduced in the related work, there are plenty of advanced technologies and systems that solve the NLOS problem. Several of these advancements can potentially enhance the performance of our system. For instance, leveraging additional features and employing feature processing techniques, implementing filter technology, and integrating other technologies such as LiDAR [16] are avenues we identify as future plans to enhance our system's performance.

7 CONCLUSION

We propose RefLoc, which leverages the assistance of LOS anchor links to address the NLOS issue for UWB localization. We find that while NLOS links of UWB may vary significantly in the same environment, LOS links can possess very similar features due to the high bandwidth of UWB. We leverage the links of anchors to infer the NLOS link for localization tags, and thus improve the localization performance. We address the practical challenges of deriving the anchor link status, ranking feature qualities, and identifying tag links. We implement RefLoc on DW1000 and design a UWB badge for real applications. Extensive evaluations in various environments show that RefLoc achieves an average identification accuracy of 96% and a 90% localization error of 0.42 m in NLOS conditions. We believe RefLoc can be a lightweight and scalable solution to improve the performance of practical UWB localization systems.

REFERENCES

[1] [n. d.]. Chi-squared test. Retrieved from https://en.wikipedia.org/wiki/Chi-squared_test

[2] [n. d.]. Dimension4 UWB RTLS. Retrieved from https://ubisense.com/dimension4/

[3] [n. d.]. Humatics Rail Navigation System. Retrieved from https://timedomain.com/products/humatics-rail-navigation-system/

[4] 2014. Channel Effects on Communications Range and Time Stamp Accuracy in DW1000 Based Systems. Retrieved from https://www.decawave.com/wp-content/uploads/2018/10/APS006_Part-1-Channel-Effects-on-Range-Accuracy_v1.03.pdf

[5] 2016. DW1000 Metrics for Estimation of Non Line Of Sight Operating Conditions. Retrieved from https://www.decawave.com/wp-content/uploads/2018/10/APS006_Part-3-DW1000-Diagnostics-for-NLOS-Channels_v1.1.pdf

[6] 2019. DW1000 User Manual. Retrieved from https://www.decawave.com/wp-content/uploads/2019/07/DW1000-User-Manual-1.pdf

[7] 2020. AirTags: Everything We Know So Far. Retrieved from https://www.macrumors.com/guide/airtags/

[8] R. W. Schafer, A. V. Oppenheim, and J. R. Buck. 1989. Discrete-time signal processing. *Prentice-Hall, Englewood Cliffs* (1989).

[9] Amr Alanwar, Henrique Ferraz, Kevin Hsieh, Rohit Thazhath, Paul Martin, João Hespanha, and Mani Srivastava. 2017. D-SLATS: Distributed simultaneous localization and time synchronization. In *Proceedings of ACM MobiHoc*.

[10] Abbas Albaidhani, Antoni Morell, and Jose Lopez Vicario. 2016. Ranging in UWB using commercial radio modules: Experimental validation and NLOS mitigation. In *Proceedings of IEEE IPIN*.

[11] Alireza Ansaripour, Milad Heydariaan, Omprakash Gnawali, and Kyungki Kim. 2020. VIPER: Vehicle pose estimation using ultra-wideband radios. In *2020 16th International Conference on Distributed Computing in Sensor Systems (DCOSS)*. IEEE, 120–127.

[12] Valentín Barral, Carlos J. Escudero, José A. García-Naya, and Roberto Maneiro-Catoira. 2019. NLOS identification and mitigation using low-cost UWB devices. *Sensors* (2019).

[13] Joan Borras, Paul Hatrack, and Narayan B. Mandayam. 1998. Decision theoretic framework for NLOS identification. In *Proceedings of IEEE Vehicular Technology*. IEEE.

[14] Klemen Bregar and Mihael Mohorčič. 2018. Improving indoor localization using convolutional neural networks on computationally restricted devices. *IEEE Access* (2018).

[15] Pi-Chun Chen. 1999. A non-line-of-sight error mitigation algorithm in location estimation. In *Proceedings of IEEE WCNC*.

[16] Zhijian Chen, Aigong Xu, Xin Sui, Yuting Hao, Cong Zhang, and Zhengxu Shi. 2022. NLOS identification- and correction-focused fusion of UWB and LiDAR-SLAM based on factor graph optimization for high-precision positioning with reduced drift. *Remote Sensing* 14, 17 (2022), 4258.

[17] Pablo Corbalán, Gian Pietro Picco, and Sameera Palipana. 2019. Chorus: UWB concurrent transmissions for GPS-like passive localization of countless targets. In *Proceedings of ACM/IEEE IPSN*.

[18] Alessio Serrani. 2019. NLOS identification and mitigation in a real time indoor Ultra Wide Band localization system. Phdthesis. Politecnico di Torino.

[19] François Despaux, Adrien Van den Bossche, Katia Jaffrès-Runser, and Thierry Val. 2018. N-TWR: An accurate time-of-flight-based N-ary ranging protocol for ultra-wide band. *Ad Hoc Networks* 79 (2018), 1–19.

[20] Carmelo Di Franco, Amanda Prorok, Nikolay Atanasov, Benjamin Kempke, Prabal Dutta, Vijay Kumar, and George J. Pappas. 2017. Calibration-free network localization using non-line-of-sight ultra-wideband measurements. In *Proceedings of IEEE IPSN*.

[21] Han Ding, Jinsong Han, Chen Qian, Fu Xiao, Ge Wang, Nan Yang, Wei Xi, and Jian Xiao. 2018. Trio: Utilizing tag interference for refined localization of passive RFID. In *Proceedings of IEEE INFOCOM*. IEEE, 828–836.
[22] Mengyao Dong. 2021. A low-cost NLOS identification and mitigation method for UWB ranging in static and dynamic environments. *IEEE Communications Letters* (2021).
[23] Mahmoud Elsanhoury, Petteri Makela, Janne Koljonen, Petri Valisuo, Ahm Shamsuzzoha, Timo Mantere, Mohammed Elmusrati, and Heidi Kuusniemi. 2022. Precision positioning for smart logistics using ultra-wideband technology-based indoor navigation: A review. *IEEE Access* 10 (2022), 44413–44445.
[24] Ruixin Fan and Xin Du. 2022. NLOS error mitigation using weighted least squares and Kalman filter in UWB positioning. *arXiv preprint arXiv:2205.05939* (2022).
[25] André G. Ferreira, Duarte Fernandes, Sérgio Branco, André Paulo Catarino, and João L. Monteiro. 2021. Feature selection for real-time NLOS identification and mitigation for body-mounted UWB transceivers. *IEEE Transactions on Instrumentation and Measurement* 70 (2021), 1–10.
[26] Nakul Garg, Yang Bai, and Nirupam Roy. 2021. Owlet: Enabling spatial information in ubiquitous acoustic devices. In *Proceedings of ACM MobiSys*.
[27] Mahanth Gowda, Ashutosh Dhekne, Sheng Shen, Romit Roy Choudhury, Lei Yang, Suresh Golwalkar, and Alexander Essanian. 2017. Bringing IoT to sports analytics. In *Proceedings of USENIX NSDI*.
[28] Bernhard Groβwindhager, Michael Stocker, Michael Rath, Carlo Alberto Boano, and Kay Römer. 2019. SnapLoc: An ultra-fast UWB-based indoor localization system for an unlimited number of tags. In *Proceedings of ACM/IEEE IPSN*.
[29] Bernhard Groβwindhager, Michael Stocker, Michael Rath, Carlo Alberto Boano, and Kay Römer. 2019. SnapLoc: An ultra-fast UWB-based indoor localization system for an unlimited number of tags. In *Proceedings of ACM/IEEE IPSN*.
[30] Bernhard Großwindhager, Michael Rath, Josef Kulmer, Mustafa S. Bakr, Carlo Alberto Boano, Klaus Witrisal, and Kay Römer. 2018. SALMA: UWB-based single-anchor localization system using multipath assistance. In *Proceedings of ACM SenSys*.
[31] IEEE 802 Working Group et al. 2011. IEEE standard for local and metropolitan area networksPart 15.4: Low-rate wireless personal area networks (LR-WPANs). *IEEE Std* (2011).
[32] Karthikeyan Gururaj, Anojh Kumaran Rajendra, Yang Song, Choi Look Law, and Guofa Cai. 2017. Real-time identification of NLOS range measurements for enhanced UWB localization. In *2017 International Conference on Indoor Positioning and Indoor Navigation (IPIN)*. IEEE, 1–7.
[33] Ismail Guvenc, Chia-Chin Chong, and Fujio Watanabe. 2007. NLOS identification and mitigation for UWB localization systems. In *Proceedings of IEEE Wireless Communications and Networking Conference*.
[34] Jinsong Han, Chen Qian, Xing Wang, Dan Ma, Jizhong Zhao, Wei Xi, Zhiping Jiang, and Zhi Wang. 2016. Twins: Device-free object tracking using passive tags. *IEEE/ACM Transactions on Networking* 24, 3 (June 2016), 1605–1617. https://doi.org/10.1109/TNET.2015.2429657
[35] Milad Heydariaan, Hossein Dabirian, and Omprakash Gnawali. 2020. Anguloc: Concurrent angle of arrival estimation for indoor localization with UWB radios. In *Proceedings of IEEE DCOSS*.
[36] Chen Huang, Andreas F. Molisch, Ruisi He, Rui Wang, Pan Tang, Bo Ai, and Zhangdui Zhong. 2020. Machine learning-enabled LOS/NLOS identification for MIMO systems in dynamic environments. *IEEE Transactions on Wireless Communications* 19, 6 (2020), 3643–3657.
[37] Yi Jiang and Victor C. M. Leung. 2007. An asymmetric double sided two-way ranging for crystal offset. In *Proceedings of IEEE Symposium on Signals, Systems and Electronics*.
[38] Zhi-Ping Jiang, Wei Xi, Xiangyang Li, Shaojie Tang, Ji-Zhong Zhao, Jin-Song Han, Kun Zhao, Zhi Wang, and Bo Xiao. 2014. Communicating is crowdsourcing: Wi-Fi indoor localization with CSI-based speed estimation. *Journal of Computer Science and Technology* 29, 4 (2014), 589–604.
[39] Kevin Jiokeng, Gentian Jakllari, Alain Tchana, and André-Luc Beylot. 2020. When FTM discovered MUSIC: Accurate WiFi-based ranging in the presence of multipath. In *Proceedings of IEEE INFOCOM*.
[40] Benjamin Kempke, Pat Pannuto, Bradford Campbell, and Prabal Dutta. 2016. Surepoint: Exploiting ultra wideband flooding and diversity to provide robust, scalable, high-fidelity indoor localization. In *Proceedings of ACM SenSys*.
[41] Jasurbek Khodjaev, Yongwan Park, and Aamir Saeed Malik. 2010. Survey of NLOS identification and error mitigation problems in UWB-based positioning algorithms for dense environments. *Annals of Telecommunications-Annales Des Télécommunications* (2010).
[42] Dae-Ho Kim, Goo-Rak Kwon, Jae-Young Pyun, and Jong-Woo Kim. 2018. NLOS identification in UWB channel for indoor positioning. In *2018 15th IEEE Annual Consumer Communications & Networking Conference (CCNC)*. IEEE, 1–4.
[43] Manikanta Kotaru, Kiran Joshi, Dinesh Bharadia, and Sachin Katti. 2015. SpotFi: Decimeter level localization using WiFi. In *Proceedings of ACM SIGCOMM*. ACM, 269–282.
[44] Ye-Sheng Kuo, Pat Pannuto, Ko-Jen Hsiao, and Prabal Dutta. 2014. Luxapose: Indoor positioning with mobile phones and visible light. In *Proceedings of the ACM MobiCom*.

[45] Bao Long Le, Kazi Ahmed, and Hiroyuki Tsuji. 2003. Mobile location estimator with NLOS mitigation using Kalman filtering. In *Proceedings of IEEE WCNC*.
[46] Vu Anh Minh Le, Matteo Trobinger, Davide Vecchia, and Gian Pietro Picco. 2022. Human occlusion in ultra-wideband ranging: What can the radio do for you? In *Proceedings of IEEE MSN*.
[47] Lingkun Li, Pengjin Xie, and Jiliang Wang. 2018. RainbowLight: Towards low cost ambient light positioning with mobile phones. In *Proceedings of the ACM MobiCom*.
[48] Weijie Li, Tingting Zhang, and Qinyu Zhang. 2013. Experimental researches on an UWB NLOS identification method based on machine learning. In *Proceedings of IEEE International Conference on Communication Technology*.
[49] Ze Li, Zengshan Tian, Mu Zhou, Zhenyuan Zhang, and Yue Jin. 2018. An accurate and robust environment sensing algorithm for enhancing indoor localization. In *Proceedings of IEEE INFOCOM*.
[50] Manni Liu, Linsong Cheng, Kun Qian, Jiliang Wang, Jin Wang, and Yunhao Liu. 2020. Indoor acoustic localization: a survey. *Human-centric Computing and Information Sciences* 10, 1 (Jan. 2020), 2.
[51] Meiyu Liu, Xizhong Lou, Xiaoping Jin, Ruwen Jiang, Kaifeng Ye, and Shubin Wang. 2021. NLOS identification for localization based on the application of UWB. *Wireless Personal Communications* 119 (2021), 3651–3670.
[52] Qingzhi Liu, Zhendong Yin, Yanlong Zhao, Zhilu Wu, and Mingyang Wu. 2022. UWB LOS/NLOS identification in multiple indoor environments using deep learning methods. *Physical Communication* 52 (2022), 101695.
[53] Yunhao Liu, Yiyang Zhao, Lei Chen, Jian Pei, and Jinsong Han. 2012. Mining frequent trajectory patterns for activity monitoring using radio frequency tag arrays. *IEEE Transactions on Parallel and Distributed Systems* 23, 11 (Nov. 2012), 2138–2149.
[54] Junhai Luo, Liying Fan, and Husheng Li. 2017. Indoor positioning systems based on visible light communication: State of the art. *IEEE Communications Surveys & Tutorials* 19, 4 (2017), 2871–2893.
[55] Dimitrios Lymberopoulos and Jie Liu. 2017. The Microsoft indoor localization competition: Experiences and lessons learned. *IEEE Signal Processing Magazine* (2017).
[56] Valerio Magnago, Pablo Corbalán, Gian Pietro Picco, Luigi Palopoli, and Daniele Fontanelli. 2019. Robot localization via odometry-assisted ultra-wideband ranging with stochastic guarantees. In *Proceedings of IEEE IROS*.
[57] Hessam Mohammadmoradi, Milad Heydariaan, Omprakash Gnawali, and Kyungki Kim. 2019. UWB-based single-anchor indoor localization using reflected multipath components. In *2019 International Conference on Computing, Networking and Communications (ICNC)*. IEEE, 308–312.
[58] Dries Neirynck, Eric Luk, and Michael McLaughlin. 2016. An alternative double-sided two-way ranging method. In *Proceedings of IEEE WPNC*. IEEE.
[59] Pat Pannuto, Benjamin Kempke, and Prabal Dutta. 2018. Slocalization: Sub-uW ultra wideband backscatter localization. In *Proceedings of ACM/IEEE IPSN*.
[60] JiWoong Park, SungChan Nam, HongBeom Choi, YoungEun Ko, and Young-Bae Ko. 2020. Improving deep learning-based UWB LOS/NLOS identification with transfer learning: An empirical approach. *Electronics* 9, 10 (2020), 1714.
[61] Ioannis Pefkianakis and Kyu-Han Kim. 2018. Accurate 3D localization for 60 GHz networks. In *Proceedings ACM SenSys*.
[62] V. Ch. Sekhar Rao Rayavarapu and Arunanshu Mahapatro. 2022. NLOS identification and mitigation in UWB positioning with bagging-based ensembled classifiers. *Annals of Telecommunications* 77, 5-6 (2022), 267–280.
[63] Maurizio Rea, Aymen Fakhreddine, Domenico Giustiniano, and Vincent Lenders. 2017. Filtering noisy 802.11 time-of-flight ranging measurements from commoditized WiFi radios. *IEEE/ACM Transactions on Networking* (2017).
[64] Matteo Ridolfi, Abdil Kaya, Rafael Berkvens, Maarten Weyn, Wout Joseph, and Eli De Poorter. 2021. Self-calibration and collaborative localization for UWB positioning systems: A survey and future research directions. *Comput. Surveys* 54, 4 (May 2021), 88:1–88:27.
[65] Cung Lian Sang, Bastian Steinhagen, Jonas Dominik Homburg, Michael Adams, Marc Hesse, and Ulrich Rückert. 2020. Identification of NLOS and multi-path conditions in UWB localization using machine learning methods. *Applied Sciences* (2020).
[66] Bo Song, Sheng-Lin Li, Mian Tan, and Qing-Hui Ren. 2018. A fast imbalanced binary classification approach to NLOS identification in UWB positioning. *Mathematical Problems in Engineering* (2018).
[67] Michael Stocker, Markus Gallacher, Carlo Alberto Boano, and Kay Römer. 2021. Performance of support vector regression in correcting UWB ranging measurements under LOS/NLOS conditions. In *Proceedings of the Workshop on Benchmarking Cyber-Physical Systems and Internet of Things*. 6–11.
[68] Chao Tang, Yinqiu Xia, and Lihua Dou. 2023. Mobility prediction based tracking of moving objects in wireless sensor networks. *Chinese Journal of Electronics* 32 (2023), 793.
[69] D. Tse and P. Viswanath. 2005. Fundamentals of wireless communication. *Cambridge University Press* (2005).
[70] Swaroop Venkatesh and R. Michael Buehrer. 2007. NLOS mitigation using linear programming in ultrawideband location-aware networks. *IEEE Transactions on Vehicular Technology* (2007).

[71] Saipradeep Venkatraman, James Caffery, and H.-R. You. 2002. Location using LOS range estimation in NLOS environments. In *Proceedings of IEEE Vehicular Technology*.
[72] Maximilian von Tschirschnitz, Marcel Wagner, Marc-Oliver Pahl, and Georg Carle. 2019. Clock error analysis of common time of flight based positioning methods. In *2019 International Conference on Indoor Positioning and Indoor Navigation (IPIN)*. IEEE, 1–8.
[73] Bowen Wang, Haixin Song, Woogeun Rhee, and Zhihua Wang. 2022. Overview of ultra-wideband transceivers–system architectures and applications. *Tsinghua Science and Technology* 27, 3 (2022), 481–494.
[74] Ju Wang, Hongbo Jiang, Jie Xiong, Kyle Jamieson, Xiaojiang Chen, Dingyi Fang, and Binbin Xie. 2016. LiFS: Low human-effort, device-free localization with fine-grained subcarrier information. In *Proceedings of ACM MobiCom*. ACM, 243–256.
[75] Ju Wang, Jie Xiong, Hongbo Jiang, Xiaojiang Chen, and Dingyi Fang. 2016. D-Watch: Embracing "bad" multipaths for device-free localization with COTS RFID devices. In *Proceedings of ACM CoNEXT*. ACM, 253–266.
[76] Tianyu Wang, Hanying Zhao, and Yuan Shen. 2020. An efficient single-anchor localization method using ultra-wide bandwidth systems. *Applied Sciences* (2020).
[77] Junyu Wei, Haowen Wang, Shaojing Su, Ying Tang, Xiaojun Guo, and Xiaoyong Sun. 2022. NLOS identification using parallel deep learning model and time-frequency information in UWB-based positioning system. *Measurement* 195 (2022), 111191.
[78] Chenshu Wu, Zheng Yang, Zimu Zhou, Kun Qian, Yunhao Liu, and Mingyan Liu. 2015. PhaseU: Real-time LOS identification with WiFi. In *Proceedings of IEEE INFOCOM*.
[79] Pengjin Xie, Lingkun Li, Jiliang Wang, and Yunhao Liu. 2020. LiTag: Localization and posture estimation with passive visible light tags. In *Proceedings of ACM SenSys (SenSys'20)*.
[80] Chouchang Yang and Huai-rong Shao. 2015. WiFi-based indoor positioning. *IEEE Communications Magazine* 53, 3 (March 2015), 150–157.
[81] Kegen Yu and Y. Jay Guo. 2007. NLOS error mitigation for mobile location estimation in wireless networks. In *Proceedings of IEEE Vehicular Technology*.
[82] Kegen Yu, Kai Wen, Yingbing Li, Shuai Zhang, and Kefei Zhang. 2018. A novel NLOS mitigation algorithm for UWB localization in harsh indoor environments. *IEEE Transactions on Vehicular Technology* (2018).
[83] Faheem Zafari, Athanasios Gkelias, and Kin K. Leung. 2019. A survey of indoor localization systems and technologies. *IEEE Communications Surveys & Tutorials* 21, 3 (April 2019), 2568–2599.
[84] Reza Zandian and Ulf Witkowski. 2018. NLOS detection and mitigation in differential localization topologies based on UWB devices. In *Proceedings of IEEE IPIN*.
[85] Zhuoqi Zeng, Rubing Bai, Lei Wang, and Steven Liu. 2019. NLOS identification and mitigation based on CIR with particle filter. In *2019 IEEE Wireless Communications and Networking Conference (WCNC)*. IEEE, 1–6.
[86] Zhuoqi Zeng, Steven Liu, and Lei Wang. 2019. UWB NLOS identification with feature combination selection based on genetic algorithm. In *2019 IEEE International Conference on Consumer Electronics (ICCE)*. IEEE, 1–5.
[87] Yunting Zhang, Zhao Wang, Weiyi Wang, Zhenge Guo, and Jiliang Wang. 2017. SOLO: 2D localization with single sound source and single microphone. In *2017 IEEE 23rd International Conference on Parallel and Distributed Systems (ICPADS)*. 787–790.
[88] Minghui Zhao, Tyler Chang, Aditya Arun, Roshan Ayyalasomayajula, Chi Zhang, and Dinesh Bharadia. 2021. ULoc: Low-power, scalable and cm-accurate UWB-tag localization and tracking for indoor applications. *Proceedings of the ACM on Interactive, Mobile, Wearable and Ubiquitous Technologies* 5, 3 (2021), 1–31.
[89] Zimu Zhou, Zheng Yang, Chenshu Wu, Wei Sun, and Yunhao Liu. 2014. LiFi: Line-of-sight identification with WiFi. In *Proceedings of IEEE INFOCOM*.
[90] Hongzi Zhu, Yuxiao Zhang, Zifan Liu, Xiao Wang, Shan Chang, and Yingying Chen. 2021. Localizing acoustic objects on a single phone. *IEEE/ACM Transactions on Networking* (May 2021), 1–14.
[91] Xiaomin Zhu, Jianjun Yi, Junyi Cheng, and Liang He. 2020. Adapted error map based mobile robot UWB indoor positioning. *IEEE Transactions on Instrumentation and Measurement* (2020).
[92] Yuan Zhuang, Chongyang Zhang, Jianzhu Huai, You Li, Liang Chen, and Ruizhi Chen. 2022. Bluetooth localization technology: Principles, applications, and future trends. *IEEE Internet of Things Journal* 9, 23 (Dec. 2022), 23506–23524.

Received 10 December 2023; revised 7 March 2024; accepted 25 March 2024